Article

The Conformational Free Energy Landscape of β-d-Glucopyranose. Implications for Substrate Preactivation in β-Glucoside Hydrolases

Xevi Biarns, Albert Ardvol, Antoni Planas, Carme Rovira, Alessandro Laio, and Michele Parrinello

J. Am. Chem. Soc., **2007**, 129 (35), 10686-10693• DOI: 10.1021/ja068411o • Publication Date (Web): 14 August 2007

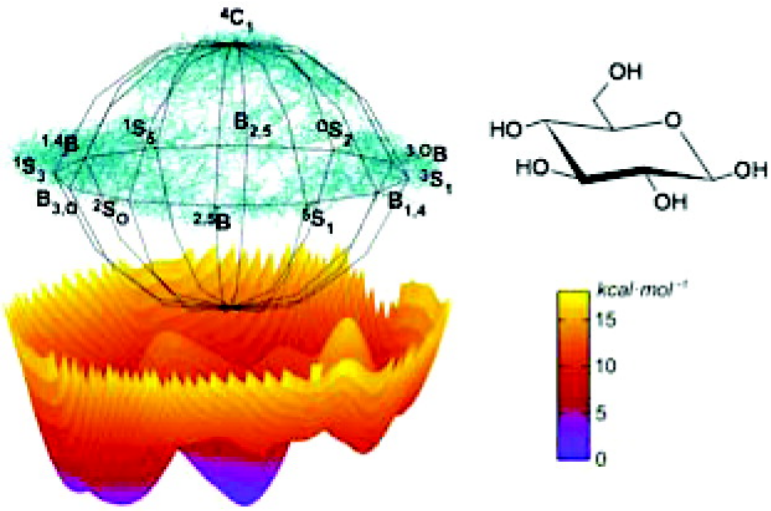

More About This Article

Additional resources and features associated with this article are available within the HTML version:

- Supporting Information
- Links to the 6 articles that cite this article, as of the time of this article download
- Access to high resolution figures
- Links to articles and content related to this article
- Copyright permission to reproduce figures and/or text from this article

View the Full Text HTML

J|A|C|S
ARTICLES
Published on Web 08/14/2007

The Conformational Free Energy Landscape of β-D-Glucopyranose. Implications for Substrate Preactivation in β-Glucoside Hydrolases

Xevi Biarnés,[†] Albert Ardèvol,[†,‡] Antoni Planas,[‡] Carme Rovira,*[,†,§] Alessandro Laio,[||] and Michele Parrinello[⊥]

Contribution from the Centre especial de Recerca en Química Teòrica, Parc Científic de Barcelona, Josep Samitier 1-5, 08028 Barcelona, Spain, Laboratory of Biochemistry, Institut Químic de Sarrià, Universitat Ramon Llull, Via Augusta, 390, 08017 Barcelona, Spain, Institució Catalana de Recerca i Estudis Avançats (ICREA), Passeig Lluís Companys, 23, 08018 Barcelona, Spain, International School for Advanced Studies (SISSA), Via Beirut 2-4, I-34014 Trieste, Italy, and Computational Science, Department of Chemistry and Applied Biosciences, ETH Zurich, USI Campus, Via Giuseppe Buffi 13, CH-6900 Lugano, Switzerland

Received November 23, 2006; E-mail: crovira@pcb.ub.es

Abstract: Using ab initio metadynamics we have computed the conformational free energy landscape of β-D-glucopyranose as a function of the puckering coordinates. We show that the correspondence between the free energy and the Stoddard's pseudorotational itinerary for the system is rather poor. The number of free energy minima (9) is smaller than the number of ideal structures (13). Moreover, only six minima correspond to a canonical conformation. The structural features, the electronic properties, and the relative stability of the predicted conformers permit the rationalization of the occurrence of distorted sugar conformations in all the available X-ray structures of β-glucoside hydrolase Michaelis complexes. We show that these enzymes recognize the most stable distorted conformers of the isolated substrate and at the same time the ones better prepared for catalysis in terms of bond elongation/shrinking and charge distribution. This suggests that the factors governing the distortions present in these complexes are largely dictated by the intrinsic properties of a single glucose unit.

1. Introduction

Carbohydrates play an essential role in life. Oligo and polysaccharides, as well as the carbohydrate moieties of glycoproteins, glucolipids and other glycoconjugates have specific roles in a variety of biological processes including cell−cell interactions, cell adhesion, modulation of growth factor receptors, inmune defense, inflammation, and viral and parasitic infections.[1]

Glycoside hydrolases (GHs) or glycosidases are the enzymes responsible for the degradation or hydrolysis of glycosidic bonds in carbohydrates.[2] Their structures are understood at the molecular level and mechanistic issues are being probed by means of the specific design and synthesis of oligosaccharide mimics.[3−6] Despite the large number of known GHs, classified into more than 100 families,[7,8] their catalytic mechanisms are similar. They typically operate by means of acid/base catalysis with retention or inversion of the anomeric configuration, although a different mechanism has recently been proposed for GH family 4.[9]

During the past decade there has been increasing evidence that several GHs are adapted to recognize energetically higher conformations of carbohydrate units before hydrolysis (see Figure 1).[10−12] In particular, for pyranoses, the saccharide unit binding at subsite −1 adopts a distorted (boat or skew) conformation instead of the relaxed $^4C_1$ chair conformation. This has been observed in several complexes of retaining and inverting GHs, as well as carbohydrate-bound biological receptors.[13,14] It has been shown that this kind of saccharide ring distortion

[†] Parc Científic de Barcelona.
[‡] Institut Químic de Sarrià.
[§] Institució Catalana de Recerca i Estudis Avançats (ICREA).
[||] International School for Advanced Studies (SISSA).
[⊥] ETH Zurich.

(1) Hurtley, S., Service, R., Szuromi, P., Eds. *Science* **2001**, *291*, 2263−2502.
(2) Davies, G.; Henrissat, B. *Structure* **1995**, *3*, 853−859.
(3) Sinnott, M. L. *Chem. Rev.* **1990**, *90*, 1171−1202.
(4) Davies, G.; Sinnott, M. L.; Withers, S. G. Glycosyl Transfer. In *Comprehensive Biological Catalysis;* Sinnott, M. L., Ed.; Academic Press Ltd.: San Diego, CA, 1998; Chapter 3, pp 119−209.
(5) Heightman, T. D.; Vasella, A. *Angew. Chem., Int. Ed.* **1999**, *38*, 750−770.
(6) Zechel, D. L.; Withers, S. G. *Acc. Chem. Res.* **2000**, *33*, 11−18.
(7) *Carbohydrate-Active enZYmes.* http://afmb.cnrs-mrs.fr/cazy/CAZY/index.html.
(8) Coutinho, P. M.; Henrissat, B. Carbohydrate-active enzymes: An integrated database approach. In *Recent Advances in Carbohydrate Bioengineering.* Gilbert, H. J., Davies, G. J., Henrissat, B., Svensson, B., Eds.; The Royal Society of Chemistry: Cambridge, U.K., 1999.
(9) Yip, V. L. Y.; Varrot, A.; Davies, G. J.; Rajan, S. S.; Yang, X.; Thompson, J.; Anderson, W. F.; Withers, S. G. *J. Am. Chem. Soc.* **2004**, *126*, 8354−8355.
(10) Davies, G. J.; Ducros, V. M.-A.; Varrot, A.; Zechel, D. L. *Biochem. Soc. Trans.* **2003**, *31*, 523−527.
(11) Taylor, E. J.; Goyal, A.; Guerreiro, C. I. P. D.; Prates, J. A. M.; Money, V.; Ferry, N.; Morland, C.; Planas, A.; Macdonald, J. A.; Stick, R. V.; Gilbert, H. J.; Fontes, C. M. G. A.; Davies, G. J. *J. Biol. Chem.* **2005**, *280*, 32761−32767.
(12) Money, V. A.; Smith, N. L.; Scaffidi, A.; Stick, R. V.; Gilbert, H. J.; Davies, G. J. *Angew. Chem., Int. Ed.* **2006**, *45*, 5136−5140.

10.1021/ja068411o CCC: $37.00

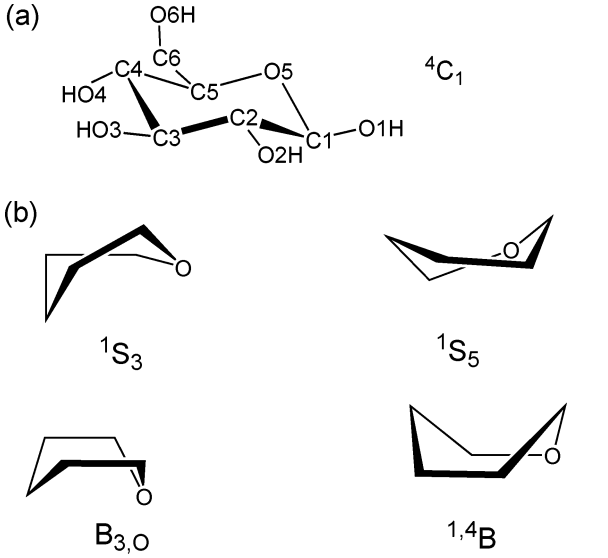

Figure 1. Ring conformations adopted by β-glucose in different glycoside hydrolases.

has favorable mechanistic consequences in glycoside hydrolysis. In particular, the distortion places the glycosidic oxygen near the acid/base catalytic residue. It also reduces the steric interaction between the hydrogen at the anomeric carbon (C1) and the nucleophile, and places the 1-O_x group (i.e., the leaving group) in a pseudoaxial position that facilitates nucleophilic attack on the anomeric carbon[15] and the subsequent cleavage of the glycosidic bond. These distortions in the Michaelis complex are therefore in the pathway to reach the transition state of the reaction, which is known to have oxocarbenium ion character.[6] Therefore, the internal conformation of a single carbohydrate unit determines its efficiency in the degradation of polysaccharides.

To classify the conformation of the substrate along the reaction pathway in several GHs according to the available crystallographic data, Davies et al.[10,12] recently used a diagram showing all the accessible conformations of a pyranoside ring (Figure 2). This diagram, proposed by Stoddart a long time ago,[16] shows schematically all the accessible conformers for a single β-glucopyranose unit, according to their corresponding IUPAC nomenclature.[17] In the following, we will refer to this diagram as Stoddart's diagram (Figure 2).[18] Apart from the chair conformation ($^4C_1$), six boat-type conformers are present as well as six skew-type conformers. Transient structures from the $^4C_1$ chair conformation to the boat/skew region (namely half-chair and envelope conformers) are also expected.

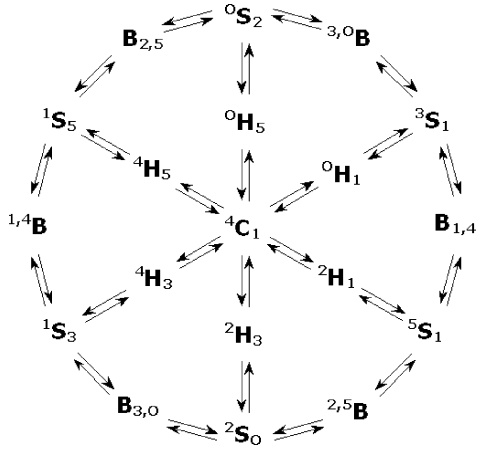

Figure 2. Stoddart's diagram.

Stoddart's diagram is often used as an "itinerary map", since it gives an idea of the possible conformational routes that might be followed by a pyranoside ring as it moves from one conformation to another. However, it gives no information as to the relative stability of the different ring conformations, nor can it be assumed that all conformations contained in the diagram correspond to stationary points on the free energy surface with respect to ring distortions. A detailed description of the free energy pathways between all the conformations of Stoddart's diagram would be useful, for instance, to understand the amount of energy that the substrate needs to acquire to reach a given distorted conformation and the electronic changes associated to the distortion. Representing the relative energy of sugar ring conformations in terms of Stoddart diagram is of interest given the wide use of this diagram in studies of GH reaction mechanisms.[10−12] It is also interesting to investigate whether the carbohydrate conformations found in X-ray analyses of E•S complexes of β-GHs have any correspondence with the stationary points of the free energy landscape of β-D-glucopyranose.

There have been many attempts to quantify energy differences among glucopyranose ring conformations using different theoretical approaches.[19] Most of these calculations are based on the use of force fields and thus electronic rearrangements cannot be analyzed. In recent years, density functional theory (DFT) has shown itself to be a powerful technique to address this and related issues.[20] However, because of the complexity of the potential energy surface of β-glucose,[21,22] these analyses have

(13) Biarnés, X.; Nieto, J.; Planas, A.; Rovira, C. *J. Biol. Chem.* **2006**, *281*, 1432−1441 and references therein.
(14) Nerinckx, W.; Desmet, T.; Claeyssens, M. *Arkivoc* **2006**, *13*, 90−116 and references therein.
(15) Kirby, A. J. Stereoelectronic effects on acetal hydrolysis. *Acc. Chem. Res.* **1984**, *17*, 305−311.
(16) Stoddart, J. F. In *Stereochemistry of Carbohydrates*; Wiley-Interscience: Toronto, Canada, 1971.
(17) (a) IUPAC-IUP Joint Commission on Biochemical Nomenclature. *Arch. Biochem. Biophys.* **1981**, *207*, 469−472. (b) The names C, B, S stand for chair, boat, and skew, respectively. Each ring structure has four atoms that approximately define a plane. The first numeral (sometimes written as superscript) indicates the number of the ring carbon atom above the plane, and the second numeral (subscript) indicates the number of the ring carbon atom below the plane.
(18) It should be noted that the actual diagram proposed by Stoddart is more extensive than the one shown in Figure 1, since it covers not only the conformers around $^4C_1$ (projection of the sphere of Figure 2 taken from the north pole) but also the ones around $^1C_4$ (projection from the south pole). In this work we focus on the North pole projection because the substrate distortions found in all the currently available structures of Michaelis complexes of β-glucoside hydrolases belong to this projection.
(19) See for instance: (a) Jeffrey, G.; Taylor, R. *J. Comput. Chem.* **1980**, *1*, 99−109. (b) Woods, R.; Szarek, W.; Smith, V. A. *J. Chem. Soc., Chem. Commun.* **1991**, *5*, 334−337. (c) McNamara, J. P.; Muslim, A.-M.; Abdel-Aal, H.; Wang, H.; Mohr, M.; Hillier, I. H.; Bryce, R. A. *Chem. Phys. Lett.* **2004**, *394*, 429−436. (d) Brady, J. W. *J. Am. Chem. Soc.* **1986**, *108*, 8153−8160. (e) Ha, S.; Gao, J.; Tidor, B.; Brady, J. W.; Karplus, M. *J. Am. Chem. Soc.* **1991**, *113*, 1553−1557. (f) Barrows, S. E.; Storer, J. W.; Cramer, C. J.; French, A. D.; Truhlar, D. G. *J. Comput. Chem.* **1998**, *19*, 1111−1129. (g) Barrows, S. E.; Dulles, F. J.; Cramer, C. J.; French, A. D.; Truhlar, D. G. *Carbohydr. Res.* **1995**, *276*, 219−251.
(20) (a) Tvaroska, I.; André, I.; Carver, J. P. *J. Am. Chem. Soc.* **2000**, *122*, 8762−8776. (b) Molteni, C.; Parrinello, M. *Chem. Phys. Lett.* **1997**, *275*, 409−413. (c) Molteni, C.; Parrinello, M. *J. Am. Chem. Soc.* **1998**, *120*, 2168−2171. (d) Fernández-Alonso, M. C.; Cañada, J.; Jiménez-Barbero, J.; Cuevas, G. *ChemPhysChem.* **2005**, *6*, 671−680.
(21) Cramer, C. J.; Truhlar, D. G. *J. Am. Chem. Soc.* **1993**, *115*, 5745−5753.
(22) Concerning the difficulty of exploring all conformations of the exocyclic groups for other sugar rings see for instance: (a) Stortz, C. A. *Carbohydr. Res.* **1999**, *322*, 77−86. (b) Schnupf, U.; Willett, J. L.; Bosma, W. B.; Momany, F. A. *Carbohydr. Res.* **2007**, *342*, 196−216.

typically been limited to a set of conformations (boats, skews, and chairs)[22−24] or to a single itinerary connecting a few conformers, such as the one leading to chair inversion.[25a] Energy changes with respect to hydroxymethyl rotation and the configuration at the anomeric carbon have also been analyzed in detail.[19f,g,20c,26b−d] Joshi and Rao presented a potential energy surface (PES) for α- and β-D-glucopyranose at the rigid-bond approximation using standard pair-interaction potentials.[26] Later on, Dowd et al. analyzed the PES for several aldopyranosyl rings,[28] including α- and β-D-glucopyranose, by means of the MM3 molecular mechanics algorithm. Complementing these previous studies, we here present a free energy landscape of the skeleton of a glucopyranose unit, corresponding to Stoddart's diagram. The free energy with our approach takes into account (except for sampling errors) the full configurational contribution, including conformational transitions of the side groups. Our calculations are based on Car—Parrinello molecular dynamics (CPMD), combined with the recently developed metadynamics approach, which is aimed at enhancing the sampling of the phase space and at mapping the free energy landscape as a function of a small number of collective variables. We here use, as collective variables, the puckering coordinates introduced by Cremer and Pople[29] and we reconstruct the equivalent free energy map of Stoddart's diagram for β-D-glucopyranose. We also analyze the structural and electronic rearrangements along the conformational itinerary. Finally, the distorted conformations observed in the E·S complexes of β-GHs are analyzed in relation to our results.

2. Methods

2.1. Puckering Coordinates. In 1975 Cremer and Pople introduced a set of puckering coordinates to unequivocally describe the conformation of any ring of any size.[29] The conformation of a six-membered ring (such as β-glucopyranose) is defined by three coordinates: a radius Q and two phase angles ϕ and θ. The Q coordinate is the sum of the perpendicular distance of each ring atom (j) to the ring average plane ($Q = \sum_j^6 z_j$). The ϕ and θ coordinates are obtained by solving the following system of equations.

$$\begin{cases} Q \sin\theta \cos\phi = \sqrt{\frac{1}{3}} \sum_{j=1}^{6} z_j \cos\left[\frac{2\pi}{6} 2(j-1)\right] \\ Q \sin\theta \sin\phi = \sqrt{\frac{1}{3}} \sum_{j=1}^{6} z_j \sin\left[\frac{2\pi}{6} 2(j-1)\right] \\ Q \cos\theta = \sqrt{\frac{1}{6}} \sum_{j=1}^{6} (-1)^{j-1} z_j \end{cases}$$

All the possible conformations of a pyranose ring unit show small variations of Q (see later) in comparison with variations of ϕ and θ.

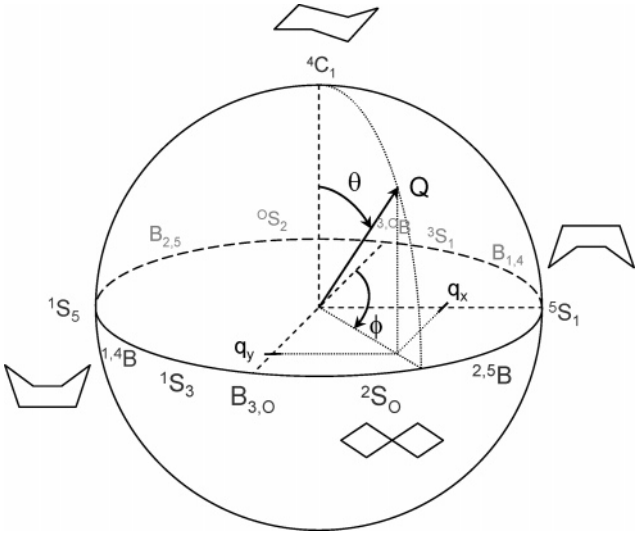

Figure 3. Cremer and Pople puckering coordinates of a six-membered ring (Q, θ and ϕ) and collective variables used in the metadynamics run (q_x and q_y).

The latter are the ones that differentiate between all the conformers of Figure 1. In fact, all the different conformers represented in Figure 1 are located on the external shell of an ellipsoid of radius Q (see Figure 3). On the poles ($\theta = 0$ or π) are located the two chair conformers ($^4C_1$ and $^1C_4$, respectively); on the equatorial region ($\theta = \pi/2$) the six boat and six skew structures are sequentially placed in steps of $\phi = \pi/6$. The Cremer and Pople puckering coordinates have been proven to be a very useful tool to analyze the conformational space of ring structures from a theoretical point of view.[14,19f,26a,b,d,e,30] Stoddart's pseudorotational itinerary (Figure 2) corresponds to the projection of the Cremer and Pople sphere (Figure 3) from the north pole. This projection can be computed in terms of the Cremer and Pople puckering coordinates as[29]

$$q_x = Q \sin(\theta) \sin(\phi)$$

$$q_y = Q \sin(\theta) \cos(\phi)$$

The two-dimensional projection (q_x, q_y) of the spherical representation of the pyranose ring conformational space (Q, θ, ϕ) facilitates the plotting and visualization of the computed free energy surface in a continuous space. We use the methodology outlined in the next section to compute the conformational free energy of β-D-glucopyranose as a function of the Cartesian coordinates q_x and q_y which allows us to sample Stoddart's diagram.

2.2. Metadynamics. Metadynamics[31] is a molecular dynamics technique aimed at enhancing the sampling of the phase space and at estimating the free energy landscape. The method is based on a dimension reduction: a set of collective variables, which enclose the essential modes that are associated with the transitions in the analyzed process, are defined (in our case, q_x and q_y). Small repulsive potential terms (Gaussian-like potentials) are added in the regions of the space that have already been explored. These repulsive potentials make the system escape from already visited points to others, as soon as biasing

(23) O'Donoghue, P.; Luthey-Schulten, Z. A. *J. Phys. Chem. B* **2000**, *104*, 10398−10405.
(24) Appell, M.; Strati, G.; Willett, J. L.; Momany, F. A. *Carbohydr. Res.* **2004**, *339*, 537−551.
(25) Momany, F. A.; Appell, M.; Strati, G.; Willett, J. L. *Carbohydr. Res.* **2004**, *339*, 553−567.
(26) (a) Ionescu, A. R.; Berces, A.; Zgierski, M. Z.; Whitfield, D. M.; Nukada, T. *J. Phys. Chem. A* **2005**, *109*, 8096−8105. (b) Kurihara, Y.; Ueda, K. *Carbohyd. Res.* **2006**, *341*, 2565−2574. (c) Momany, F. A.; Appell, M.; Willett, J. L.; Schnupt, U.; Bosma, W. B. *Carbohydr. Res.* **2006**, *341*, 525−537. (d) Karamat, S.; Fabian, W. M. F. *J. Phys. Chem. A* **2006**, *110*, 7477−7484. (e) French, A. D.; Dowd, M. K. *J. Mol. Struct. (Theochem)* **1997**, *395*−*396*, 271−287.
(27) Joshi, N.; Rao, V. S. *Biopolymers* **1979**, *18*, 2993−3004.
(28) Dowd, M. K.; French, A. D.; Reilly, P. J. *Carbohydr. Res.* **1994**, *264*, 1−19.
(29) Cremer, D.; Pople, J. A. *J. Am. Chem. Soc.* **1975**, *97*, 1354−1358.
(30) (a) Haasnoot, C. A. G. *J. Am. Chem. Soc.* **1992**, *114*, 882−887. (b) Rao, V. S.; Chandrasekaran, R.; Qasba, P. K.; Balaji, P. V. *Conformation of Carbohydrates*; Harwood Academic Publishers: Amsterdam, The Netherlands, 1998; p 56. (c) French, A. D.; Brady, J. W. *ACS Symp. Ser.* **1990**, *430*, 120−140.
(31) (a) Ensing, B.; De Vivo, M.; Liu, Z. W.; Moore, P.; Klein, M. L. *Acc. Chem. Res.* **2006**, *39*, 73−81. (b) Ensing, B.; Laio, A.; Parrinello, M.; Klein, M. L. *J. Phys. Chem.* **2005**, *109*, 6676−6687. (c) Laio, A.; Rodriguez-Fortea, A.; Gervasio, F. L.; Ceccarelli, M.; Parrinello, M. *J. Phys. Chem. B* **2005**, *109*, 6714−6721.

potential counterbalances the underlying free energy.[32] The method can be exploited for accelerating rare events, but also for mapping the free energy surface, which can be estimated as the negative of the sum of the Gaussian potential terms. This method has recently been applied to a variety of problems in the areas of biophysics, chemistry, and material science.[33]

The two coordinates chosen for this study (q_x and q_y) fulfill the requirements for suitable collective variables in the metadynamics procedure:[28] (i) they are explicit functions of the atomic positions, and (ii) they are able to distinguish the different states of the system (i.e., all conformers in Stoddart's diagram). Even though no constraint was imposed on the movement along the sphere (Figure 2), only the northern hemisphere was sampled, indicating that the energy barriers associated to the north−south transitions are higher than the ones within the northern hemisphere.

2.3. Simulation Details. The metadynamics simulations were done within the Car−Parrinello approach, as described in ref 34. In this scheme, the Car−Parrinello Lagrangian[35] is extended by extra terms describing the fictitious dynamics of the collective variables. These additional fictitious particles are coupled (through a harmonic potential) to the value of the selected collective variables in the real system.[34] The mass for this fictitious particle and the force constant of the coupling potential were tested to ensure that the coupled particle follows naturally the value of the associated collective variable in the real system. Values of 10 amu for the mass of the fictitious particle and 0.2 au for the force constant were found to fulfill these conditions. The dynamics of the fictitious particle is biased by the sequential addition of repulsive Gaussian-like potentials, which prevent the fictitious system from revisiting previously sampled configurations, and hence forces the system to escape from one minimum to another. The height of these Gaussian terms was set at 0.3 kcal mol^{-1}, which ensures sufficient accuracy for the reconstruction of the free energy surface.[31] The width of the Gaussian terms was set at 0.15 Å according to the oscillations of the selected collective variables observed in a free dynamics. A new Gaussian-like potential was added every 100 MD steps. To explore completely the free energy landscape (13 different conformations) it was necessary to add 3700 Gaussians. In terms of simulation time this corresponds to 3.7×10^5 MD steps (44.4 ps).

The system analyzed consists of a single glucopyranose unit (24 atoms) enclosed in an orthorhombic box of size 12 Å × 11 Å × 13 Å periodically repeated in space. The Kohn−Sham orbitals are expanded in a plane wave (PW) basis set with a kinetic energy cutoff of 70 Ry. Ab initio pseudopotentials were employed, generated within the Troullier−Martins scheme.[36] The calculations were performed using the Perdew, Burke, and Ernzerhoff generalized gradient-corrected approximation (PBE).[37] This functional form has been proven to give a good performance in the description of hydrogen bonds[38] and was already used in our previous work on the Michaelis complex of 1,3−1,4-β-glucanase.[13] The fictitious mass for the electronic degrees of freedom of the CP Lagrangian was set at 850 au, and the simulation time step at 0.12 fs. The starting structure for the simulation corresponds to a $^4C_1$ chair conformation. This structure was equilibrated at 300 K for 2 ps before starting the metadynamics run.

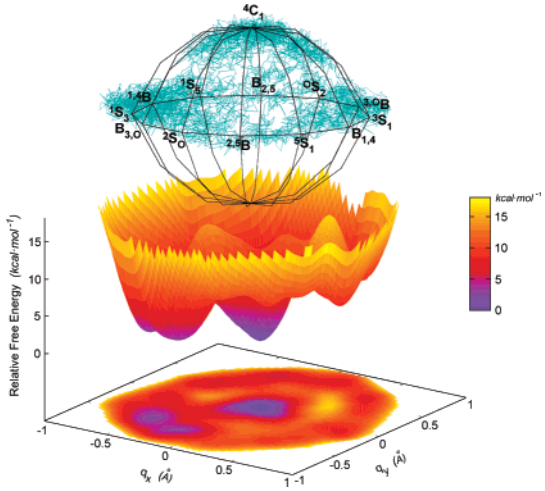

Figure 4. Trajectory of the metadynamics simulation projected on the conformational sphere of Figure 3. The reconstructed free energy landscape is shown below the figure.

To test the energy dependence on the exchange-correlation functional, additional calculations were performed on a few minima of the free energy surface (M1, M3, and M8, defined later on) using different exchange-correlation functionals (Becke−Perdew and B3LYP). These calculations were performed using the 6-31+G* basis set. The order of stability of the minima was found to be independent of the functional employed and the relative energies varied by ±0.6 kcal/mol. The relative energies computed for these structures are in reasonable agreement with the ones reported in previous studies of the potential energy surface of glucopyranose. The study of Dowd et al.[28] reports 6.51 kcal/mol for the ^2S_O structure, above the most stable chair conformer. The lowest B3LYP/6-311++G** relative energy of Appell et al.[26] for a nonchair β-glucose structure, corresponding to an intermediate between $B_{3,O}$ and ^2S_O, is 4.75 kcal/mol (in terms of ΔE) and 3.4 kcal/mol (in terms of ΔG). Our CPMD calculations give 4.12 kcal/mol (ΔE) and 3.0 kcal/mol (ΔG), respectively, for the $B_{3,O}/^2S_O$ conformer (M3).

3. Results and Discussion

The trajectory of the system along the metadynamics simulation, projected on the conformational sphere, is shown in Figure 4. All conformations belonging to the northern hemisphere were sampled, and the reconstructed free energy landscape is shown below it. Further details of the trajectory are provided in the Supporting Information (SI). Analysis of the conformation of the exocyclic groups (four −OH and one $-CH_2OH$) during the metadynamics simulation (Figures S1, S2, and Table S1 in the SI) shows that the four hydroxyl groups sample several different conformations, while the hydroxymethyl group is mainly in the *gg* orientation during the simulation. Other orientations, *tg* and *gt* are also explored but are less populated. This indicates that the free energy estimated by metadynamics takes into account also the different conformations of the exocyclic groups, although statistical errors due to the finite simulation time cannot be excluded.

The projection of the free energy landscape over the q_x-q_y plane is shown with more detail in Figure 5. The corresponding representation in terms of the θ and ϕ puckering coordinates is provided in the SI (pages 5−6). Each point in the diagram corresponds to a different ring conformation. For the sake of clarity, we have labeled the minima according to their stability

(32) Laio, A.; Parrinello, M. *Proc. Nat. Acad. Sci. U.S.A.* **2002**, *99*, 12562−12566.
(33) Recent applications include: (a) Blumberger, J.; Ensing, B.; Klein, M. L. *Angew. Chem., Int. Ed.* **2006**, *45*, 2893−2897. (b) Fiorin, G.; Pastore, A.; Carloni, P.; Parrinello, M. *Biophys. J.* **2006**, *91*, 2768−2777. (c) Martoñak, R.; Donadio, D.; Oganov, A. R.; Parrinello, M. *Nat. Mater.* **2006**, *5*, 623−626. (d) Oganov, A. R.; Martoñak, R.; Laio, A.; Raiteri, P.; Parrinello, M. *Nature* **2005**, *438*, 1142−1144. (e) Rodriguez-Fortea, A.; Iannuzzi, M.; Parrinello, M. *J. Phys. Chem. B* **2006**, *110*, 3477−3484. (f) Rodriguez-Fortea, A.; Iannuzzi, M.; Parrinello, M. *J. Phys. Chem. C* **2007**, ASAP.
(34) Iannuzzi, M.; Laio, A.; Parrinello, M. *Phys. Rev. Lett.* **2003**, *90*, 238302-(4).
(35) Car, R.; Parrinello, M. *Phys. Rev. Lett.* **1985**, *55*, 2471−2474.
(36) Troullier, M.; Martins, J. L. *Phys. Rev. B* **1991**, *43*, 1993−2006.
(37) Perdew, J. P.; Burke, K.; Ernzerhof, M. *Phys. Rev. Lett.* **1996**, *77*, 3865−3868. Erratum: *Phys. Rev. Lett.* **1997**, *78*, 1396.
(38) Ireta, J.; Neugebauer, J.; Sheffler, M. *J. Phys. Chem. A* **2004**, *108*, 5692−5698.

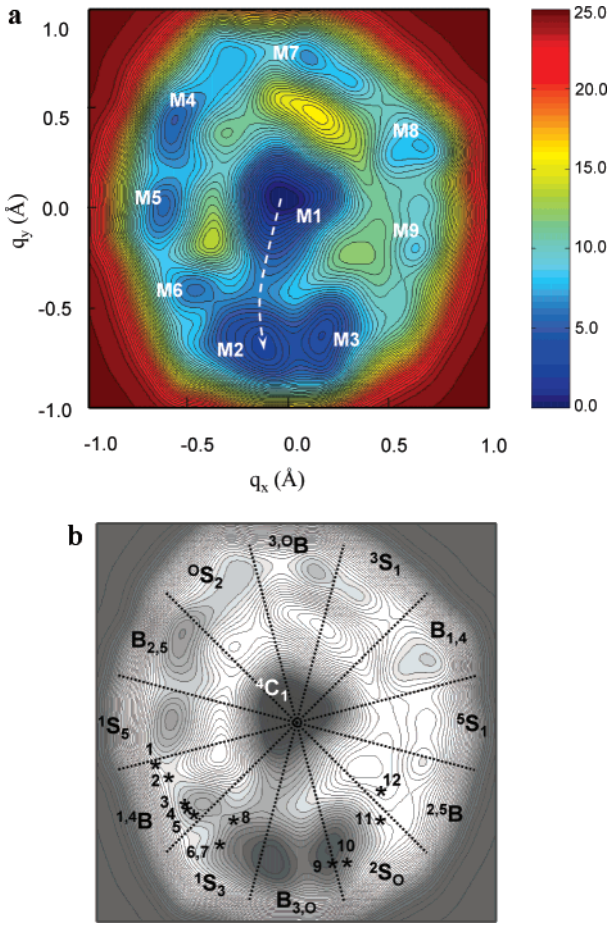

Figure 5. (a) Computed free energy landscape of β-D-glucopyranose with respect to ring distortion. Energy values are given in kcal/mol and each contour line of the diagram corresponds to 0.5 kcal/mol. (b) Distribution of the canonical conformations of the contour of Stoddart's diagram (Figure 2) on the computed free energy surface, according to the values of the ϕ puckering coordinate. The dashed lines, separated by 30° in ϕ, indicate regions corresponding to the different canonical conformations. The conformations found in experimental structures of glucoside hydrolase Michaelis complexes (Table 2) are represented by star symbols, following the numbering defined in Table 2.

Table 1. Relative Energies (E_{rel}, in kcal mol^{-1}) among the Main Stationary Points of the Free Energy Landscape (see Figure 5a)

minimum	q_x	q_y	conformation	E_{rel}
M1	0.00	0.06	$^{4}C_1$	0.0
M2	−0.45	−0.53	$B_{3,O}$	2.6
M3	−0.18	−0.63	$B_{3,O}$ / $^{2}S_O$	3.0
M4	−0.28	0.67	$B_{2,5}$	5.5
M5	−0.54	0.32	$^{1}S_5$	5.8
M6	−0.61	−0.12	$^{1,4}B/^{1}S_3$	6.3
M7	0.46	0.61	$^{3,O}B$	7.2
M8	0.72	−0.05	$B_{1,4}$	7.9
M9	0.45	−0.49	$^{2,5}B/^{5}S_1$	9.0

(from M1 to M9). As expected, the most stable conformer is the $^{4}C_1$ chair (M1 in Figure 5a). There are two local minima (M2 and M3) at ~3 kcal mol^{-1} above it and six other local minima (M4, M5, M6, M7, M8, and M9) which are more than 5 kcal mol^{-1} higher in free energy (see Table 1). It is also apparent from Figure 5a that the most stable distorted conformations (M2−M5) fall on one half of the diagram, while the other half contains the shallowest minima. Interconversion from M1 to any of the other local minima involves energetic barriers ≥8 kcal mol^{-1}.

It is interesting to relate the computed free energy landscape (Figure 5a) with the ideal diagram given by Stoddart representation (Figure 2). This can be done by dividing the surface in 12 radial regions according to the ϕ puckering coordinate (Figure 3). Each region corresponds to one of the 12 different canonical conformations of the contour of Stoddart diagram, as shown in Figure 5b. We assume that a local minimum corresponds to a canonical conformation when it is enclosed between its two nearest division lines. Intermediate conformations are assigned to minima located within $\phi \pm 7°$ around a division line. As expected from previous works,[27,28] not all stationary points have a direct correspondence with the conformations represented in Stoddart's diagram. For instance, M3 corresponds to a conformation between $B_{3,O}$ and $^{2}S_O$ and M6 is between $^{1,4}B$ and $^{1}S_3$. Moreover, there is at least one canonical conformer ($^{O}S_2$) with no direct correspondence to a computed local minimum. As a consequence, there are fewer local minima (eight) than conformations in the diagram periphery (twelve).

The fact that the position of the minima deviates from each of the canonical conformations is mainly due to two factors: (a) the fact that the ring is not rigid (i.e., not all bonding distances are the same along the diagram); and (b) the presence of intramolecular interactions among the OH ring substituents (either O−H···O hydrogen bonds or H···H repulsive interactions), which ultimately influence the ring conformation. For instance, in a perfect $^{2,5}B$ conformer there is close contact between the H atoms of C2 and C6, so the ring avoids this by evolving toward a conformation between $^{2,5}B$ and $^{5}S_1$ (M9 in Figure 5a). These deviations from the canonical conformations are not a peculiarity of an isolated glucose itself but also occur for the glucose ring of enzyme-bound polysaccharides. In fact, in our previous study[13] we found that the conformation of the substrate (a 4-methylumbelliferyl tetrasaccharide) in the Michaelis complex of 1,3-1,4-β-glucanase is located between $^{1,4}B$ and $^{1}S_3$ (i.e., a conformation corresponding to M6 in Figure 5a).

To check whether there is a relation between the positions of the local minima and the occurrence of distorted sugar conformations in enzyme-bound polysaccharides, we analyzed the ring distortions occurring in Michaelis complexes of β-GHs from all available X-ray structures in which the sugar ring located at subsite −1 is a β-glucose derivative. The q_x and q_y coordinates of the saccharide at subsite −1 were computed and the corresponding value was located on the computed free energy landscape (Figure 5b). The position of the experimental points in the diagram should be viewed with caution, first because not all structures are solved with high resolution and second because all structures correspond to modified forms of either the substrate (i.e., enzyme−inhibitor complexes) or the enzyme (i.e., mutants), so that the corresponding nonmodified forms could exhibit a slightly different distortion. Nevertheless, it is clear from Figure 5b that the most commonly observed conformations fall on one-half of the diagram (between $^{1}S_5$ and $^{2,5}B$, counterclockwise). As was pointed out by Davies et al.,[10] these conformations share a common feature of having the glycosidic bond (C1−O_x) in an axial orientation (see Figure 1). This is a crucial fact that explains why these conformations are selected: since they have the leaving group in the axial position, the hydrolysis of the glycosidic bond is facilitated and the substrate is preactivated for catalysis. In addition, we have

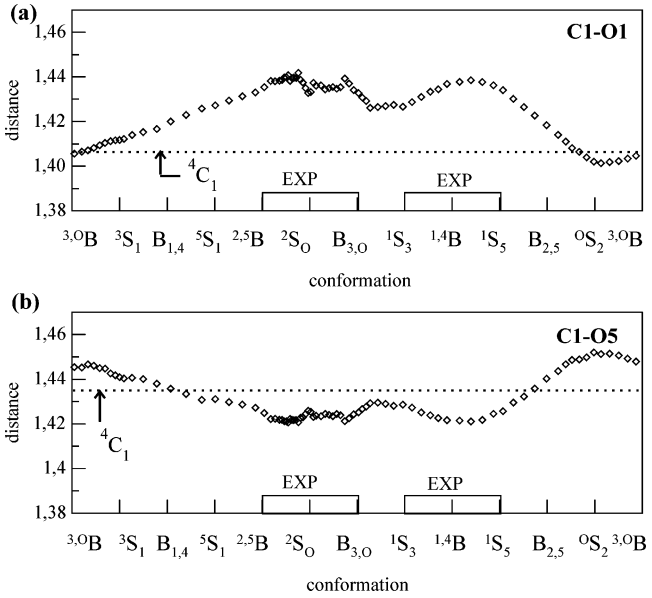

Figure 6. (a) Distance between the anomeric carbon and its substituent oxygen (C1−O1) plotted against the ring conformation (see text). A running average of each 10 data values is taken. The dotted line represents the distance obtained for the $^4C_1$ conformation using the same procedure. (b) Same analysis for the distance between the anomeric carbon and the ring oxygen (C1−O5).

found here that the region between $^1S_5$ and $^{2,5}B$ is also where the most stable distorted conformations of β-D-glucopyranose are located. Therefore, by selecting the conformations having the glycosidic bond (C1−O_x) in an axial position, the enzyme is at the same time recognizing the most stable distorted conformers of the substrate.

Analysis of the internal structure of the conformers and their electronic changes upon distortion can provide further insight into the relation between these aspects. The two most relevant structural parameters are the C1−O5 and C1−O1 distances (see Figure 1a) because these are the ones that change during catalysis[6] (viz. the C1−O5 acquires partial double bond character and the C1−O1 distance lengthens in the oxocarbenium ion-like transition state). In our previous work on the E·S complex of 1,3-1,4-β-glucanase we showed that the C1−O1 distance increases upon distortion (∼0.06 Å).[13] At the same time, the distance between the anomeric carbon and the sugar oxygen (C1−O5) decreases by a similar amount. These changes are reminiscent of the ones occurring during the enzymatic reaction, thus showing that the distortion preactivates the substrate by bringing it to a structure closer to the transition state of the reaction.

To estimate how the C1−O5 and C1−O1 distances change in the different conformations, we took a number of snapshots along the metadynamics trajectory (one every 110 fs, i.e., 46 MD steps, 120 structures) and submitted them to geometry optimization. The C1−O5 and C1−O1 distances of the optimized structure were plotted against the value of the ϕ puckering coordinate (Figure 6), which defines the conformation along the B−S itinerary in Stoddart's diagram (Figure 2). As shown in Figure 6a,b there are significant changes of the C1−O1 and C1−O5 distances with ring conformation (C1−O1 varies from 1.39 to 1.44 Å and C1−O5 varies from 1.42 to 1.46 Å). It is also clear from Figure 6 that the C1−O1 and C1−O5 distances vary in an opposite way: when C1−O1 increases, C1−O5

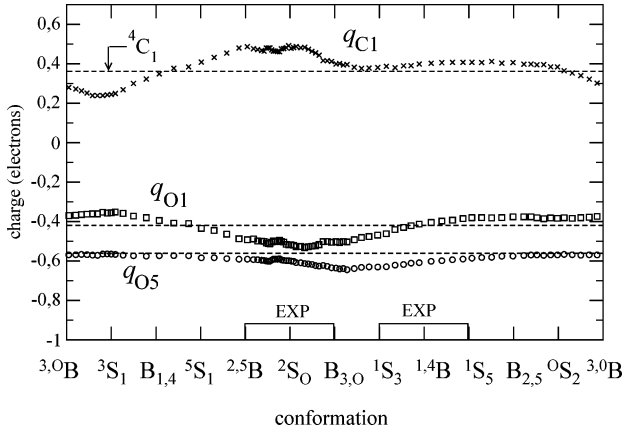

Figure 7. ESP charge on the anomeric carbon (q_{C1}), the ring oxygen (q_{O5}) and the hydroxyl oxygen of the anomeric carbon (q_{O1}) with respect to ring conformation. A running average of each 10 data values is taken. The dashed lines represent the average charge obtained for the $^4C_1$ conformation on each of the three atoms (C1, O1, and O5, from top to bottom).

decreases. In addition, the longer C1−O1 distances and shortest C1−O5 occur for the conformers located approximately on the itineraries defined by $^{2,5}B-^2S_O-B_{3,O}$ and by $^1S_3-^{1,4}B-^1S_5$. Therefore these conformers are the ones that most resemble an oxocarbenium ion. Interestingly, the conformers found in E·S complexes of β-GHs fall in these two regions (Figure 5c), suggesting that the factors governing the distortion are largely dictated by the intrinsic properties of a single glucose ring.

The electronic changes with conformation were analyzed in a similar way. The atomic ESP charges on the anomeric carbon (q_{C1}), the ring oxygen (q_{O5}) and the oxygen attached to the anomeric carbon (q_{O1}) are shown in Figure 7. The conformations having larger q_{C1} values than the $^4C_1$ chair (dashed line) are $^{2,5}B-^2S_O-B_{3,O}$ and, to a lesser extent, $^1S_3-^{1,4}B-^1S_5-B_{2,5}$. At the same time, an accumulation of negative charge on O5 and O1 is observed. Once more, these conformations approximately coincide with the most stable distorted conformations in terms of free energy (see Figure 5a). Therefore, we find that the most stable distorted conformers are those that fulfill the maximum number of structural/electronic requirements for efficient catalysis: large C1−O1/C1−O5 ratio, large q_{C1} and having 1-OH in an axial orientation.

The information obtained from the structural and electronic analysis (Figures 6 and 7), together with the list of available complexes of β-glucoside hydrolases, is summarized in Table 2. The first column lists all B and S conformers of Stoddart's diagram (Figure 2) in a consecutive order. Columns 2−4 contain the change in distances (C1−O1 and C1−O5) and charge of the anomeric carbon (q_{C1}) with respect to the values obtained for the $^4C_1$ chair conformer. The last column gives information on the different E·S complexes that have been characterized experimentally (numbered from **1** to **12**). As it is not possible

(39) Papanikolau, Y.; Prag, G.; Tavias, G.; Vorgias, C. E.; Oppenheim, A. B.; Petratos, K. *Biochemistry* **2001**, *40*, 11338−11343.
(40) Van Aalten, D. M. F.; Komander, D.; Synstad, B.; Gseidnes, S.; Peter, M. G.; Eijsink, V. G. H. *Proc. Natl. Acad. Sci. U.S.A.* **2001**, *98*, 8979−8984.
(41) Markovic-Housley, Z.; Miglierini, G.; Soldatova, L.; Rizkallah, P. J.; Muller, U.; Schirmer, T. *Struct. Fold. Des.* **2000**, *8*, 1025−1035.
(42) Sulzenbacher, G.; Driguez, H.; Henrissat, B.; Schulein, M.; Davies, G. J. *Biochemistry* **1996**, *35*, 15280−15287.
(43) Verdoucq, L.; Moriniere, J.; Bevan, D. R.; Esen, A.; Vasella, A.; Henrissat, B.; Czjzek, M. *J. Biol. Chem.* **2004**, *279*, 31796−31803.
(44) Davies, G. J.; Mackenzie, L.; Varrot, A.; Dauter, M.; Brzozowski, A. M.; Schulein, M.; Withers, S. G. *Biochemistry* **1998**, *37*, 11707−11713.

Table 2. Main Structural and Electronic Changes (δ(O1−C1) and δ(O1−C5), in Angstrom, and $\delta(q_{C1})$ in Electron Units) Associated with a Perfect Conformation of a Given Type (i.e., the Canonical Conformations of the Contour of Stoddart's Diagram)[a]

distortion	δ(C1–O1)	δ(C1–O5)	$\delta(q_{C1})$	enzyme[b] no./name/PDB code/resolution/ family /ref
$^{1}S_{5}$	+0.027	−0.010	+0.035	
	+0.031	−0.015	+0.035	**1**/Chitinase A/1eib/1.80 Å/GH 6/39
	+0.031	−0.015	+0.032	**2**/Chitinase B/1e6n/2.25 Å/GH 18/40
	+0.029	−0.015	+0.027	**3**/hyaluronidase/1fcv/2.65 Å/GH 56/41
$^{1,4}B$	+0.030	−0.015	+0.030	
	+0.028	−0.014	+0.022	**4**/endo-1,4-glucanase I/1ovw/2.7 Å/GH 7/42
	+0.027	−0.013	+0.018	**5**/cyanogenic-β-glucosidase/1v03/2.0 Å/GH 1/43
	+0.022	−0.009	+0.013	**6**/endo-1,4-glucanase/ 4a3h/1.65 Å/GH 5/44
	+0.021	−0.009	+0.013	**7**/β-glucosidase 1/1e56/2.10 Å/GH 1/45
	+0.021	−0.009	+0.013	**8**/endoglucanase/1w2u/1.52 Å/GH 12/46
$^{1}S_{3}$	+0.020	−0.008	+0.010	
$B_{3,O}$	+0.025	−0.011	+0.030	
	+0.036	−0.016	+0.086	**9**/cellobiohydrolase II/1qk2/2.0 Å/GH 6/47
	+0.037	−0.016	+0.107	**10**/cellobiohydrolase II/1gz1/1.90 Å/GH 6/47
$^{2}S_{O}$	+0.036	−0.016	+0.120	
	+0.035	−0.016	+0.126	**11**/cellobiohydrolase II/1ocn/1.31 Å/GH 6/48
	+0.031	−0.015	+0.128	**12**/endo-1,4-glucanase A/1kwf/0.94 Å/GH 8/49
$^{2,5}B$	+0.028	−0.010	+0.110	
$^{5}S_{1}$	+0.019	−0.005	+0.034	
$B_{1,4}$	+0.012	0.000	−0.030	
$^{3}S_{1}$	+0.004	+0.004	−0.130	
$^{3,O}B$	−0.002	+0.010	−0.088	
$^{O}S_{2}$	−0.006	+0.015	0.000	
$B_{2,5}$	+0.010	+0.004	+0.030	

[a] The values associated with the experimental structures are also included (see text). Positive/negative values refer to their increase/decrease with respect to the same value for the $^{4}C_{1}$ chair. The fifth column lists the available complexes of β-GHs in which the saccharide at subsite−1 adopts a given conformation (see also Figure 5b). [b] Search performed in Sept. 2006. Only E·S complexes in which the sugar ring of the subsite−1 is a glucose derivative have been considered.

to assign a particular canonical conformation to each structure in a strict sense, we have placed every experimental structure in between its closest canonical conformations (e.g., **1** is below $^{1}S_{5}$ and above $^{1,4}B$ in Table 2). The values of δ(C1−O1), δ(C1−O5), and $\delta(q_{C1})$ corresponding to the experimental structures have been obtained from Figures 6 and 7, taking into account the puckering coordinates of each E·S complex. As shown in Table 2, all experimental structures (**1**−**12**) have positive values of $\delta(q_{C1})$ (i.e., increase of charge at the anomeric carbon), positive values of δ(C1−O1) (i.e., the C1−O1 distance increases), and negative δ(C1−O5) values (C1−O5 distance decreases) with respect to the $^{4}C_{1}$ chair. Thus they fulfill the requirements for efficient catalysis.

From the results of Table 2 it is possible to predict the most suitable conformation/s for substrate preactivation. The conformations listed below $^{5}S_{1}$ do not seem to be good candidates, since they show either small changes of the relevant parameters or variations in the wrong direction. For instance, the $B_{1,4}$ conformation results in a decrease of the charge on the anomeric carbon and the $^{3}S_{1}$, $^{3,O}B$, and $^{O}S_{2}$ conformations show an increase of the C1−O5 distance. Therefore, it is not expected that the substrate in the E·S complex adopts any of the conformations listed below $^{5}S_{1}$ (i.e., $^{5}S_{1}$, $B_{1,4}$, $^{3}S_{1}$, $^{3,O}B$ and $^{O}S_{2}$). The $^{2,5}B$, $^{5}S_{1}$, $B_{2,5}$ and $^{1}S_{5}$ conformations show only moderate changes of the relevant parameters, but these are in the direction that favors substrate recognition. There is no experimental E·S complex located in the regions between $^{2,5}B-{}^{5}S_{1}$ and $B_{2,5}-{}^{1}S_{5}$ (see also Figure 5c), but we cannot exclude the possibility that some could be found. The same considerations apply to the region between $^{1}S_{3}$ and $B_{3,O}$. Instead, the conformations falling around $B_{3,O}-{}^{2}S_{O}$ and $^{1,4}B-{}^{1}S_{3}$ appear to be particularly favored as they show the largest values of δ(C1−O1), δ(C1−O5), and $\delta(q_{C1})$. Thus, a substrate adopting any of these conformations would be well prepared for the nucleophilic reaction. A similar conclusion but based on different arguments was reached by Davies et al. in their study of reaction pathways in β-GHs.[10] As discussed by the authors, those Michaelis complexes showing either $^{2}S_{O}$ or $^{1}S_{3}$ types of distortion lead to transition-state structures (e.g., $^{2,5}B$ and $^{4}H_{3}$, respectively) that fulfill the requirement of having C5−O5−C1−C2 planarity, thus showing strong oxocarbenium-ion-like character. Our results give support to these considerations. We demonstrate here that, in addition to this, in the conformations falling around $B_{3,O}-{}^{2}S_{O}$ and $^{1,4}B-{}^{1}S_{3}$ the glucose ring itself shows the largest degree of oxocarbenium-ion-like character, which in turn favors the nucleophilic attack on the anomeric carbon.

4. Summary and Conclusions

The conformational pseudorotational itinerary proposed by Stoddart[16] is commonly used to rationalize the conformation of the substrate along the reaction pathway of β-GHs.[10−12] However, it gives no information as to the relative stability of the different ring conformations nor it can be assumed that all conformations contained in the diagram correspond to minima of the free energy surface with respect to ring distortions, as pointed out in previous studies.[27,28] In this work, we have obtained the quantum mechanical free energy landscape associated with Stoddart's diagram for the simplest case of β-D-glucopyranose. Our calculations were performed by means of

(45) Czjzek, M.; Cicek, M.; Zamboni, V.; Bevan, D. R.; Henrissat, B.; Esen, A. *Proc. Natl. Acad. Sci. U.S.A.* **2000**, *97*, 13555−13560.
(46) Sandgren, M.; Berglund, G. I.; Shaw, A.; Stahlberg, J.; Kenne, L.; Desmet, T.; Mitchinson, C. *J. Mol. Biol.* **2004**, *342*, 1505−1517.
(47) Varrot, A.; Frandsen, T.; Driguez, H.; Davies, G. *Acta Crystallogr., Sect. D* **2002**, *58*, 2201−2204.
(48) Varrot, A.; Macdonald, J.; Stick, R. V.; Pell, G.; Gilbert, H. J.; Davies, G. J. *Chem. Commun.* **2003**, *21*, 946−947.
(49) Guerin, D. M.; Lascombe, M. B.; Costabel, M.; Souchon, H.; Lamzin, V.; Beguin, P.; Alzari, P. M. *J. Mol. Biol.* **2002**, *316*, 1061−1069.

Car−Parrinello molecular dynamics, using the recently developed metadynamics approach and adapting the puckering coordinates introduced by Cremer and Pople[29] as collective variables. The free energy with our approach takes into account (except for sampling errors) the full configurational contribution, including conformational transitions of the side groups. In addition, since a quantum-mechanical methodology is used, electronic rearrangements and changes in the intramolecular distances upon ring conformation are available at each point of Stoddart's diagram.

The computed free energy landscape shows eight local minima around the contour of the diagram, compared to 12 canonical conformations in Stoddart diagram. These minima are located 2.6−9.0 kcal/mol above the $^4C_1$ chair global minimum. Five of them correspond to one of the canonical conformations of Stoddart's diagram ($B_{3,O}$, $^1S_5$, $B_{2,5}$, $^{3,O}B$, and $B_{1,4}$) while the rest fall in between two canonical conformations (e.g., $B_{3,O}/^2S_O$, $^{1,4}B/^1S_3$, and $^{2,5}B/^5S_1$). The most stable minima have the 1-OH in an axial orientation and fall on one half of the diagram, similarly to what is found in X-ray structures of enzyme-bound polysaccharides of β-GHs.

Analysis of the changes in bond distances and atomic charges in the different conformers provides further insight into the question of why these conformers are found in GHs. The conformers located along $^5S_1-^{2,5}B-^2S_O-B_{3,O}$ and $^1S_3-^{1,4}B-^1S_5$ maximize the structural/electronic requirements needed for efficient catalysis: large anomeric C1−O distance, short C1−O5 distance, large charge at the anomeric carbon and having an axial 1-OH. Therefore, a substrate adopting a conformation in any of these regions would be preactivated for catalysis and it is precisely here where most of the distorted structures of Michaelis complexes of β-GHs are found. Therefore, these enzymes recognize the most stable distorted conformers of the isolated substrate and at the same time the ones better prepared for catalysis in terms of bond elongation/shrinking and charge distribution. This suggests that the factors governing the distortion are largely dictated by the intrinsic properties of a single glucose unit and that enzyme−substrate interactions have evolved to fulfill all those criteria for efficient catalysis.

Acknowledgment. This work was supported by Grants 2005SGR-00036 and 2005SGR-00883 from the Generalitat de Catalunya, FIS2005-00655 and BFU2004-06377-C02-02 from the Ministerio de Educación y Ciencia (MEC). The computer resources were provided by the Barcelona Supercomputing Center (BSC). We thank one of the referees for pointing out several aspects that were crucial to understanding this work.

Supporting Information Available: Orientation of the exocyclic groups during the metadynamics trajectory; representation of the free energy landscape in terms of the θ and ϕ puckering coordinates. This material is available free of charge via the Internet at http://pubs.acs.org.

JA068411O